Platinum electrocatalysts based on oxide supports for hydrogen and methanol fuel cells

L. A. Frolova and Yu. A. Dobrovolsky

Institute of Problems of Physical Chemistry, Russian Academy of Sciences, 1 prosp. Akad. Semenova, 142432 Chernogolovka, Moscow Region, Russian Federation. Fax: +7 (496) 522 1657. E-mail: laf@icp.ac.ru

Platinum electrocatalysts for fuel cells based on individual oxides Pt/SnO_2 and Pt/TiO_2 and their solid solutions $Pt/Ti_{1-x}M_xO_2$ (M = Ru, Nb) and $Pt/Sn_{1-x}M'_xO_{2-\delta}$ (M′ = Sb, Ru) were prepared. The influence of the composition of the oxide supports on the activity of the supported platinum catalysts in electrooxidation of methanol and hydrogen in the presence of CO was studied. The prepared platinum catalysts supported on solid solutions of tin dioxide $Sn_{1-x}M_xO_{2-\delta}$ (M = Sb, Ru; $x = 0.4$—0.9) and $Ti_{1-x}M_xO_2$ (M = Ru, Nb; $x = 0.7$) exhibited higher tolerance to CO poisoning and higher activities for methanol electrooxidation than commercial Pt,Ru catalysts on carbon support. The use of the proposed oxide supported catalysts in hydrogen and direct methanol fuel cells improved their performances in comparison with that for the fuel cells with traditional Pt,Ru catalysts on carbon support.

Key words: hydrogen and methanol fuel cell, electrocatalysts, oxide supports for electrocatalysts, electrooxidation of methanol.

Development and wide commercialization of new ecologically safe energy sources are dependent, to a considerable extent, on the state of elaborations in the area of low-temperature fuel cells (FCs) working on biofuel or syngas, which are obtained from renewable natural resources. Direct methanol FCs are especially promising power sources for portable devices. The catalysts based on superfine platinum are most efficient for the electrooxidation of hydrogen and small organic molecules.[1—5] For stabilization of nanocrystalline platinum, supports with a high surface area are usually used. Carbon materials are a common choice.[1] Unfortunately, the practical application of direct methanol FCs is still a matter of concern because of the low activity of anodic catalysts due to platinum poisoning by strongly adsorbed species (CO, formaldehyde) coming from the dissociative adsorption of the alcohol.[6,7] In addition, carbon supports do not always exhibit adequate resistance to corrosion caused by electrochemical oxidation on the fuel cell.[8—14] Platinum further accelerates the corrosion rate of carbonm leading to severe agglomeration or growth of electrocatalyst particles and thus degradation of cell performance.[1]

Catalytic systems based on alloys of other metals with Pt are developed to decrease poisoning of Pt catalysts by carbon monoxide. However, the most part of these systems, especially the systems with base metals, are poorly resistant to corrosion and, hence, the polymer membrane of these FC are easily poisoned.[9]

Another way to improvement of the catalysts for the oxidation of CO and organic fuels is the production of Pt catalysts on oxide supports, which are highly stable in an oxidative medium of FC.[15—24]

The oxide supports based on TiO_2 and SnO_2 are interesting for the development of highly active and stable electrocatalysts for PEMFC.[15—19,25—42] These supports activate electrocatalytic processes on platinum and increase its resistance to poisoning.[15—42] However, their electron conductivity is insufficiently high for the use of these compounds as electrode materials. Doping titanium and tin oxides with some elements, for example, V, Nb, Ru, Sb, and others, results in the formation of a series of solid solutions containing oxygen vacancies that enhance the electron conductivity of the support.[26—28,38]

The support nature exerts a considerable effect on both the formation of electrocatalysts and their activity and stability. The production of efficient catalytic systems with specified characteristics requires the study of the influence of introduced additives on the properties of the support surface and activity of the supported Pt catalysts.

The purpose of this work was to prepare catalysts based on platinized individual oxides Pt/SnO_2 and Pt/TiO_2 and solid solutions $Pt/Ti_{1-x}M_xO_2$ (M = Ru, Nb) and $Pt/Sn_{1-x}M'_xO_{2-\delta}$ (M′ = Sb, Ru) with different contents of the dopants. Our aim was to study the influence of their composition on the catalytic activity during the electrooxidation of methanol and hydrogen in the presence of

Published in Russian in *Izvestiya Akademii Nauk. Seriya Khimicheskaya,* No. 6, pp. 1076—1086, June, 2011.

1066-5285/11/6006-1101

CO, to compare the activities of the obtained catalytic systems, and to test the most efficient catalysts in hydrogen—air and methanol PEMFC.

Experimental

Synthesis of oxide supports and catalysts. Individual TiO_2, SnO_2, and mixed oxides $Ti_{1-x}M_xO_2$ (M = Nb, Ru) and $Sn_{1-x}M'_xO_2$ (M′ = Sb, Ru) were synthesized by the method of reversed micelles. Metal salts $SnCl_4 \cdot 5H_2O$, $SbCl_3$, $TiCl_4$, $NbCl_5$, and $RuCl_3 \cdot H_2O$ were dissolved in cyclohexane containing the corresponding amount of the surfactant (cetyltrimethylammonium bromide (CTAB)), NaOH was added to pH = 13, and after thorough stirring the mixture was stored for 1 day to form oxide particles. The obtained materials were thoroughly washed and annealed in ambient air for 2 h. The annealing temperature of SnO_2 and $Sn_{1-x}M'_xO_2$ (M′ = Sb, Ru) was 500 °C, and that of TiO_2 and $Ti_{1-x}Ru_xO_2$ was 400 °C. To increase the conductivity of $Ti_{1-x}Nb_xO_2$, this support was additionally annealed for 2 h at 400 °C in a hydrogen flow.[43]

Mixed oxides $Ti_{1-x}M_xO_2$ (M = Nb, Ru) and $Sn_{1-x}M'_xO_2$ (M′ = Sb, Ru) were obtained to study the influence of the amount of additives introduced into TiO_2 and SnO_2 on the electrophysical properties. The initial reagents were introduced in the following ratios: M′/Sn = 0.03, 0.05, and 0.10; Nb/Ti = 0.05 and 0.01; and Ru/Ti = 0.03, 0.05, and 0.10.

Platinum was introduced onto the oxide surface by the reduction of metal from a solution of H_2PtCl_6 in ethylene glycol at 160 °C in an inert atmosphere. The Pt content in the catalysts was ~10 wt.%.

Physicochemical methods. X-ray phase analyses (Thermo ARL X′TRA) were used for the characterization of the oxide supports and catalysts. The average sizes of platinum crystallites in catalysts were estimated from the broadening of the X-ray diffraction peak of Pt (111). The specific surface area of the oxides was determined using the BET method (NOVA Quantachrome 3200, inaccuracy 5%). The morphology and average particle size were analyzed by scanning (Zeiss LEO SUPRA 25) and transmission (JEM1200 EX, JEOL) electron microscopy. The composition of the samples was monitored by a JEOL JSM840A microanalyzer in a complex with the microanalytical computer system and by X-ray fluorescence analysis. The conductivity of the oxides was measured using the two-contact method in a cell with titanium electrodes in air using cyclic voltammetry (CV) and impedance spectroscopy. The impedance spectra were recorded in the frequency range from 0.014 Hz to 0.5 MHz. The amplitude of the external variable signal was 5—20 mV. A P-7S potentiostat and a Z-350m impedance meter (Elins) were used. Inaccuracies of both alternating- and direct-current measurements are caused by the determination error of geometric sizes of the determined samples and were 5%.

Electrochemical methods. Electrochemical studies of the catalysts were carried out in the standard three-electrode cell Pt//1 *M* H_2SO_4//Pt/MO_x (**1**). The normal hydrogen electrode (NHE) was used as a reference electrode.

The specific surface of active Pt in the catalysts was determined from the voltammetric curves measured in cell **1** according to a procedure[44] described previously with allowance for the value of charge consumed to CO and hydrogen desorption. Ultimately thin catalyst layers were used (the thickness and content of the catalytic layer on the electrode were ~5 μm and ~30 μg cm^{-2}, respectively), which made it possible to avoid diffusion limitations with respect to the reactant and to estimate the electrocatalytic activity of the studied samples in the kinetic region.[45] The working electrolyte was 1 *M* H_2SO_4. Cyclic voltammograms were detected in the potential range 0.03—1.0 V with the scan rate v = 50 mV s^{-1}. The experimental error of these methods for measurement of the specific surface is ~5%.

The catalytic activity of the samples was studied by chronoamperometry under the steady-state conditions using the model gas-diffusion electrode and cell **1** modeling the anode of the methanol FC according to the thin-layer method.[46,47] Solutions of 0.5 *M* CH_3OH were used in experiments.[48]

The efficiency of the active catalytic layer of the anode was estimated by the work of a membrane electrode assembly (MEA) of the FC with the solid polymer electrolyte Nafion 112 (DuPont). The catalytic layer contained a 0.05% Nafion solution mixed with low-molecular-weight alcohols (DuPont).

When preparing electrodes for electrochemical experiments, the catalyst was first mixed with the corresponding amount of a Nafion®NRE-212 solution by dispersion in an ultrasonic bath for 30 min and then supported on the surface of a gas-diffusion layer made from the Toray carbon paper. For the formation of the active catalytic layer, 10 wt.% of the ionomer Nafion were added to the platinized sample.[49] The load of platinum on the MEA electrodes for experiments with the gas mixture (H_2/CO(100 ppm)) was 0.4 mg cm^{-2}, and in the methanol FC it was 1.0 mg cm^{-2}. The relative humidity of the supplied gas mixtures (H_2/CO(100 ppm)) and air was 95%. The commercial catalyst Pt(20%)/C (E-TEK) was used in tests of catalysts in the MEA FC composition at the cathode, and the active layer of the cathode was prepared according to a standard procedure.[1] All measurements were carried out at 25 °C.

Results and Discussion

Influence of the composition of the oxide supports on their structural and electrophysical properties. *Structural and morphological properties of the oxide materials.* According to the X-ray diffraction data, the samples SnO_2, TiO_2, $Sn_{1-x}Sb_xO_2$, $Sn_{1-x}Ru_xO_2$, and $Ti_{1-x}Ru_xO_2$ represent the single phase corresponding to the rutile-like structure with the tetragonal crystalline lattice (*P*4/*mnm*) (Fig. 1, *a*). This agrees with the literature data, according to which a series of solid solutions is formed in the systems $Sn_{1-x}Sb_xO_{2-\delta}$ and $Sn_{1-x}Ru_xO_2$ at the Sb and Ru contents up to ~30 and 10 mol.%, respectively,[42,50—52] and in the system $Ti_{1-x}M_xO_2$ (at the content of M = Nb, Ru up to 10 mol.%).[31,53,54] The X-ray diffraction pattern of the sample $Ti_{1-x}Nb_xO_2$ corresponds to the X-ray diagram of the anatase phase (*I*4/*amd*) (see Fig. 1, *a*).[26,48]

The unit cell parameters were calculated for the well crystallized samples (annealing temperature ≥ 400 °C) (Table 1). The unit cell parameters of the $Sn_{1-x}Sb_xO_2$ sample increase with an increase in the antimony content. This indicates, most likely, that the oxidation state of antimony in the oxide is mainly +3.[55] In the $Ti_{1-x}Nb_xO_2$

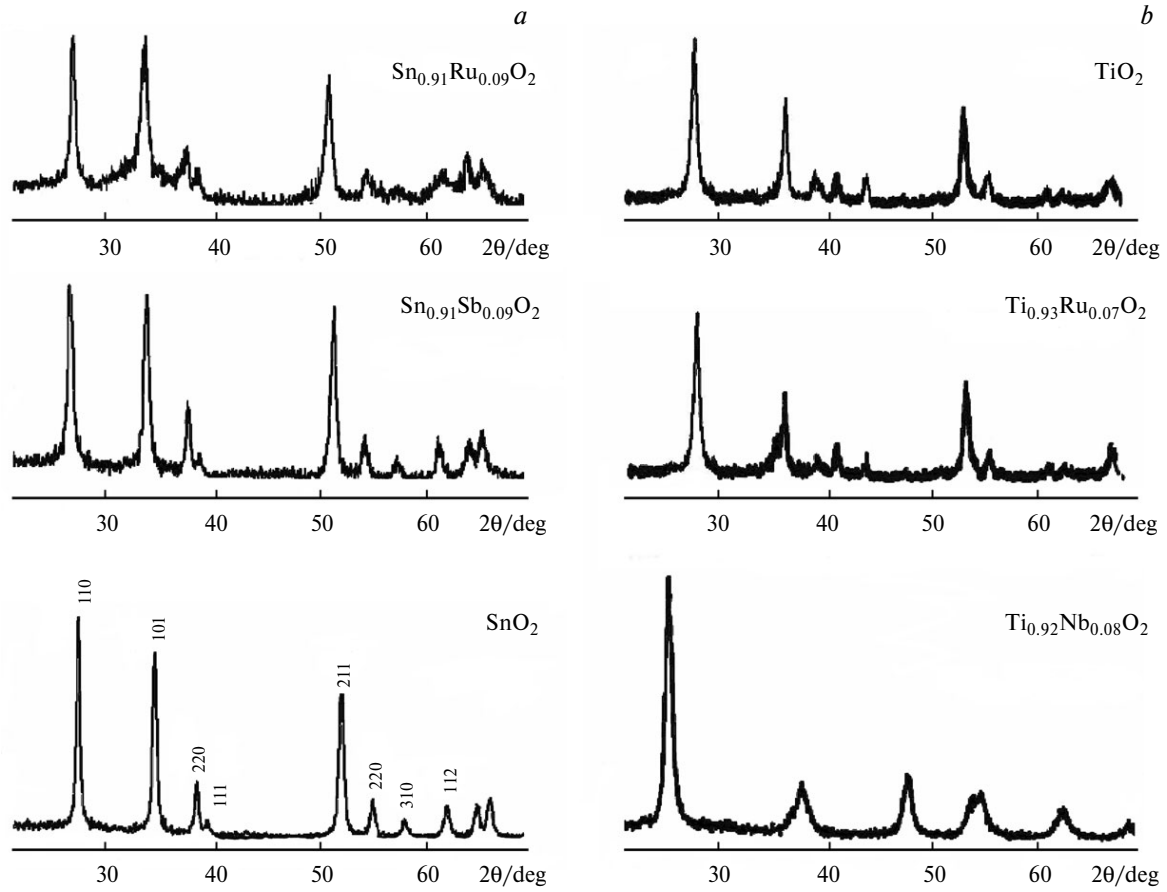

Fig. 1. X-ray diffraction patterns of the oxides $Sn_{1-x}M_xO_2$ (M = Sb, Ru) (*a*) and $Ti_{1-x}M_xO_2$ (M = Nb, Ru) (*b*) with various compositions.

samples, the unit cell parameters are also increased compared to undoped titania with the anatase structure ($a = b = 0.37864$ Å, $c = 0.94843$ Å), probably, due to the inclusion of Nb in the lattice of TiO_2.[43] For other complex oxides, the unit cell parameters do not differ within the determination error.

The values of specific surface (S_{sp}) of all prepared oxides after annealing are presented in Table 1. Their close values for various oxide materials can be explained by the common method of preparation. Some increase in S_{sp} is observed for the mixed oxide systems compared to the individual oxides.

According to the data of scanning electron microscopy, all prepared samples are characterized by the narrow particle-size distribution with an average diameter of ~20 nm (Fig. 2).

Table 1. Characteristics of the oxides of various composition

Sample	Average particle diameter/nm	$S_{sp}/m^2\,g^{-1}$*	Unit cell parameters/nm	
			a	*c*
TiO_2	20	108	0.4593±0.0001	0.2959±0.0001
SnO_2	18	102	0.4731±0.0002	0.3187±0.0002
$Sn_{1-x}Sb_xO_2$** ($x = 0.03$—0.09)	17	96—110	0.4742±0.0002	0.3192±0.0002
$Sn_{1-x}Ru_xO_2$** ($x = 0.02$—0.09)	15	102—105	0.4729±0.0002	0.3184±0.0002
$Ti_{1-x}Ru_xO_2$** ($x = 0.01$—0.07)	18	105—112	0.4594±0.0002	0.2959±0.0002
$Ti_{1-x}Nb_xO_2$** ($x = 0.04$—0.08)	20	109—115	0.3788±0.0001	0.9487±0.0001

* The error of measurement of the specific surface (S_{sp}) of the oxides is 5%.

** The crystal unit cell parameters for solid solutions did not differ within the determination error.

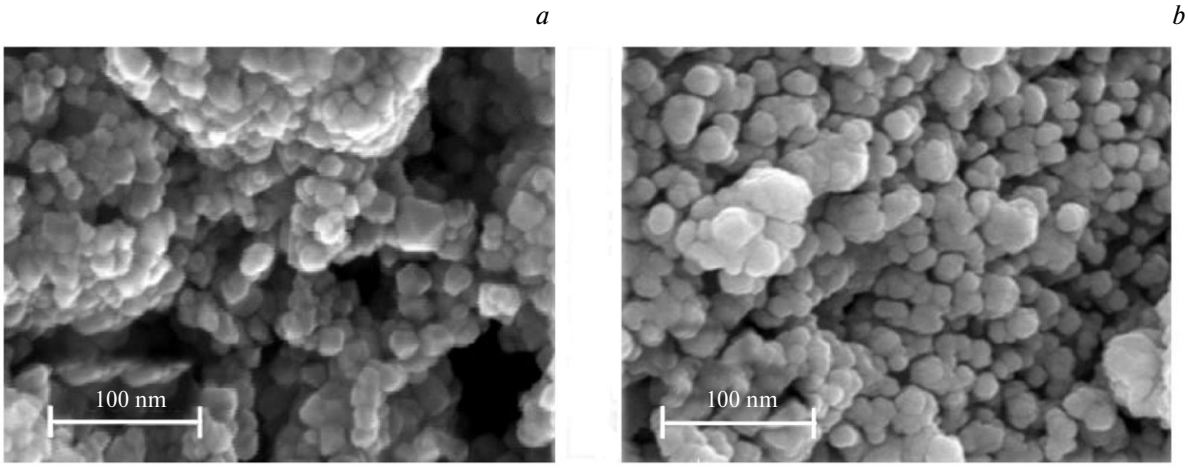

Fig. 2. Microimages of TiO_2 (*a*) and SnO_2 (*b*) after annealing.

The chemical composition of the obtained oxides is given in Table 2.

Influence of the composition of the oxide materials on the electron conductivity. The study of the dependence of the electron conductivity (σ_{el}) on the compositions of $Sn_{1-x}M'_xO_2$ (M′ = Ru, Sb) (Fig. 3, *a*) and $Ti_{1-x}M_xO_2$ (M = Nb, Ru) (Fig. 3, *b*) showed that the electron conductivity of the complex oxides increases with an increase in the amount of introduced additives. The highest values of electron conductivity (~4 $Ohm^{-1}\,cm^{-1}$) are observed for the system $Sn_{1-x}Sb_xO_{2-\delta}$ with the antimony content 4—9 mol.%. The values of σ_{el} obtained for the systems $Sn_{1-x}Sb_xO_2$ and $Ti_{1-x}Nb_xO_2$ are consistent with the published data,[26,43,50] and for $Sn_{1-x}Ru_xO_2$ they turned out to be higher than the electron conductivity obtained by other authors.[42] Individual oxides TiO_2 and SnO_2 have

Table 2. Composition and morphology of the prepared catalysts

Sample	Composition of oxides	Content of platinum (%)	d_{Pt}*/nm	
			I	II
Pt/TiO_2	TiO_2	9.54	3	6
$Pt/SnO_2/C$	SnO_2	10.10	3	5
$Pt/Sn_{1-x}Sb_xO_2$	$Sn_{0.97}Sb_{0.03}O_{2-\delta}$	8.21	4	6
	$Sn_{0.06}Sb_{0.04}O_{2-\delta}$	8.64	3	5
	$Sn_{0.91}Sb_{0.09}O_{2-\delta}$	9.01	3	6
$Pt/Sn_{1-x}Ru_xO_2$	$Sn_{0.98}Ru_{0.02}O_2$	9.72	3	7
	$Sn_{0.95}Ru_{0.05}O_2$	9.31	4	7
	$Sn_{0.91}Ru_{0.09}O_2$	9.82	3	5
$Pt/Ti_{1-x}Ru_xO_2$	$Ti_{0.99}Ru_{0.01}O_2$	8.71	4	6
	$Ti_{0.96}Ru_{0.04}O_2$	9.67	4	7
	$Ti_{0.93}Ru_{0.07}O_2$	10.05	3	6
$Pt/Ti_{1-x}Nb_xO_2$	$Ti_{0.96}Nb_{0.04}O_2$	9.34	3	7
	$Ti_{0.92}Nb_{0.08}O_2$	9.58	3	5

* Average diameter of the platinum particles obtained using electron microscopy (I) and estimated from broadening of the reflections of Pt (111) by the Sherrer equation (II).

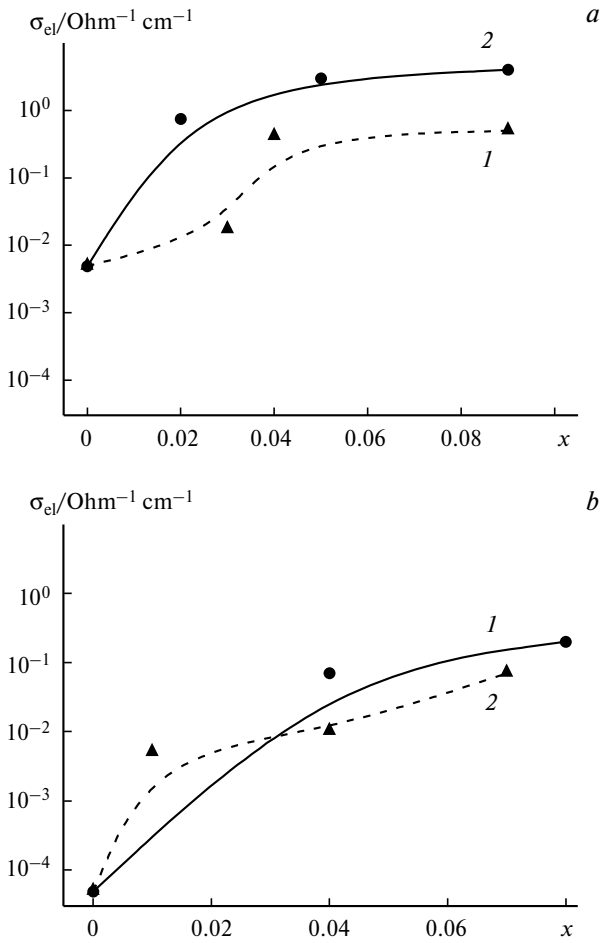

Fig. 3. Electron conductivity (σ_{el}) of the oxides $Sn_{1-x}M_xO_2$ with M = Ru (*1*) and Sb (*2*) (*a*) and $Ti_{1-x}M_xO_2$ with M = Nb (*1*) and Ru (*2*) (*b*) with various compositions.

a relatively low electron conductivity of $5.0 \cdot 10^{-8}$ and $4.7 \cdot 10^{-3}$ Ohm^{-1} cm^{-1}, respectively.

Characteristics of the catalysts Pt/oxide support. *Morphology of the catalysts*. The typical microimage of the prepared platinized oxides is presented in Fig. 4, *a*. According to electron microscopic examination, the average size of the platinum clusters in the catalysts was 2—5 nm. These data are consistent with the values of average size range of the Pt crystallites estimated by the broadening of the Pt (111) reflections in the diffraction patterns of the catalysts. The typical X-ray diffraction pattern for the metal-oxide catalyst is shown in Fig. 4. The characteristics of all catalysts prepared are listed in Table 2.

An analysis of the compositions of the samples by X-ray microanalysis and the study of the catalysts by transmission electron microscopy showed a uniform distribution of platinum over the oxide support surface with the metal content in the samples presented in Table 2.

Evaluation of the state of the catalyst surface by the CV method. The cyclic voltammograms for the prepared catalysts are shown in Fig. 5. In the case of the low electron conductivity of the supports (SnO_2, TiO_2), ~5 wt.% of carbon black were added to the catalysts. The electron conductivity of these mixtures was 0.5 Ohm^{-1} cm^{-1}.

For all catalysts prepared using the oxide supports, the CV curves had the shape characteristic of the curves for pure platinum (see Fig. 5).

For the mixed compositions $Ti_{0.91}Ru_{0.07}O_2$, $Ti_{0.92}Nb_{0.08}O_2$, and $Sn_{1-x}M_xO_2$ (M = Sb, Ru) with the content of doping components 4—9 mol.%, more intense peaks of hydrogen and oxygen adsorption/desorption are observed, which probably indicates their enhanced catalytic activity. The enhancement of the activity can be related to the influence of the support and also to an increased efficiency of electrochemical processes at the three-phase interface electrode/electrolyte/reactant (due to a lower ohmic resistance of the support). This assumption is favored by a substantial increase in the catalytic activity of the individual platinized oxides caused by addition of the electroconducting additive (carbon black) (see Fig. 5). At the same time, the addition of carbon black to the catalysts prepared using the supports with $\sigma_{el} > 0.2$ Ohm^{-1} cm^{-1} does not substantially change the shape of the CV curves. It may be concluded that the ohmic resistance of the electrodes at σ_{el} of the support ~0.2 Ohm^{-1} cm^{-1}) is rather low and does not limit the rate of the electrode processes in the kinetic regime.[49] It is most likely that for the efficient use of the catalyst the conductivity of the support in the real catalytic layer should be 10—15 times higher (~2—3 Ohm^{-1} cm^{-1}).

The fragments of the CV curves of the oxidative desorption of CO obtained for the platinized oxides with various compositions are shown in Fig. 6. The data for Pt/C (E-TEK) are presented for comparison. The shift of the peak of CO oxidative desorption to the region of lower potentials compared to Pt/C is observed for all catalysts on the oxide supports. For $Pt/Sn_{1-x}M_xO_2$ (M = Ru, Sb) this effect is more pronounced (shift by 0.10—0.15 V) and is accompanied by an increase in the specific currents of CO oxidation. Note that for the catalysts based on TiO_2 the introduction of Nb and Ru additives results in an additional decrease in the potentials of the CO desorption peak by 0.01 and 0.02 V, respectively (with respect to Pt/TiO_2). The same effect is observed for the catalysts based on tin dioxide doped with ruthenium.

Many authors believe that one of the reasons for the described phenomena is the so-called "bifunctional" mechanism. This implies that water chemisorption on the oxide surface, during which adsorbed oxygen-containing species are formed, occurs at lower potentials than that on Pt, favoring the activation of the strongly adsorbed carboxyl groups on the adjacent Pt atoms.[42,56—60]

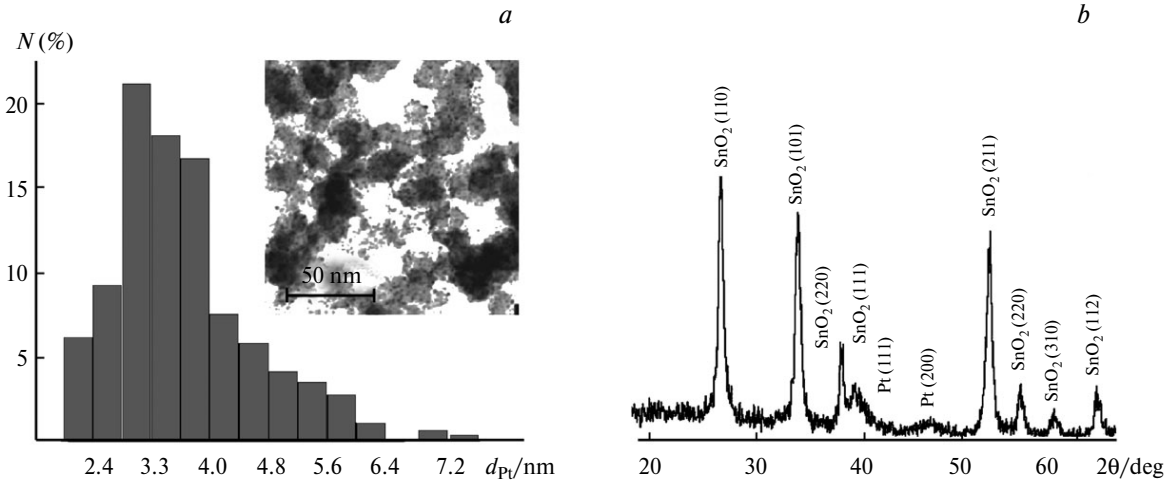

Fig. 4. Microimage (inset), the histogram of the platinum particle size distribution (*a*), and the X-ray diffraction pattern (*b*) for the catalyst Pt/SnO_2.

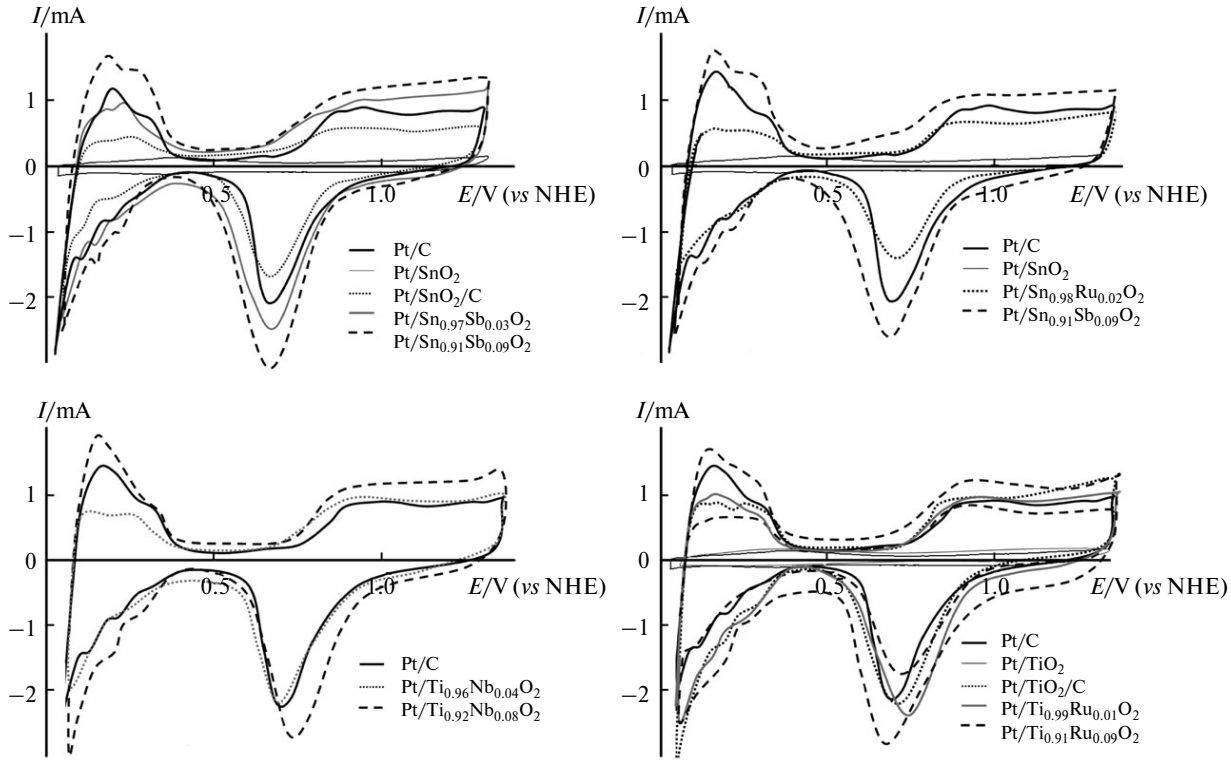

Fig. 5. CV curves of the platinized oxides with various compositions for the base electrolyte 1 *M* H_2SO_4, $v = 0.05$ V s^{-1}. The loading of the catalyst on the electrode is 30 μg cm^{-2}.

$$Pt + CO \longrightarrow Pt{-}CO_{ads},$$

$$MO_x + H_2O \longrightarrow MO_x{-}OH_{ads} + H^+ + e^-,$$

$$Pt{-}CO_{ads} + MO_x{-}OH_{ads} \longrightarrow$$

$$\longrightarrow Pt + MO_x^+ + CO_2 + H^+ + e^-. \qquad (1)$$

The values of specific active surface of the catalysts calculated with allowance for the charge consumed to the oxidative desorption of CO and hydrogen are presented in Table 3.

Similarity of the values of S_{CO} and S_H indicates that the metal-oxide catalysts undergo no serious structural distortions in the presence of CO.

Catalytic properties of the catalysts in the electrooxidation of hydrogen and CO. *Influence of the CO content in hydrogen on the stability of the catalytic properties*. The values of specific currents obtained by chronoamperometry ($E = 0.5$ V) for the oxidation of an H_2/CO(100 ppm) mixture on the catalysts with various compositions are presented in Fig. 7. The values of stationary oxidation currents for all catalysts are normalized to their specific active surface (mA cm^{-2}).

A comparison of the catalytic properties of the individual platinized oxides showed that $Pt/TiO_2/C$ exhibits a higher activity. Doped tin and titanium dioxides promoted the increase in the activity of the electrocatalysts obtained on the basis of these dioxides (see Fig. 7). The compositions $Pt/Sn_{1-x}Sb_xO_{2-\sigma}$ ($x = 0.04$, 0.09) turned out to be most efficient.

Table 3. Specific active surface of the Pt catalysts with various compositions calculated with allowance for the charge consumed to the oxidative desorption of hydrogen (I) and CO (II)*

Sample	S_{sp}/m^2 g^{-1}	
	I	II
Pt/C	46	48
$Pt/TiO_2/C$	40	38
$Pt/SnO_2/C$	25	27
$Pt/Sn_{1-x}Sb_xO_{2-\sigma}$ ($x = 0.03$)	34	36
$Pt/Sn_{1-x}Sb_xO_{2-\sigma}$ ($x = 0.04$)	60	64
$Pt/Sn_{1-x}Sb_xO_{2-\sigma}$ ($x = 0.09$)	65	68
$Pt/Sn_{1-x}Ru_xO_2$ ($x = 0.02$)	29	34
$Pt/Sn_{1-x}Ru_xO_2$ ($x = 0.05$)	55	53
$Pt/Sn_{1-x}Ru_xO_2$ ($x = 0.09$)	58	61
$Pt/Ti_{1-x}Ru_xO_2$ ($x = 0.01$)	51	54
$Pt/Ti_{1-x}Ru_xO_2$ ($x = 0.04$)	58	60
$Pt/Ti_{1-x}Ru_xO_2$ ($x = 0.07$)	65	62
$Pt/Ti_{1-x}Nb_xO_2$ ($x = 0.04$)	37	41
$Pt/Ti_{1-x}Nb_xO_2$ ($x = 0.08$)	51	54

* The experimental error of these methods for measurement of the specific surface is ~5%.

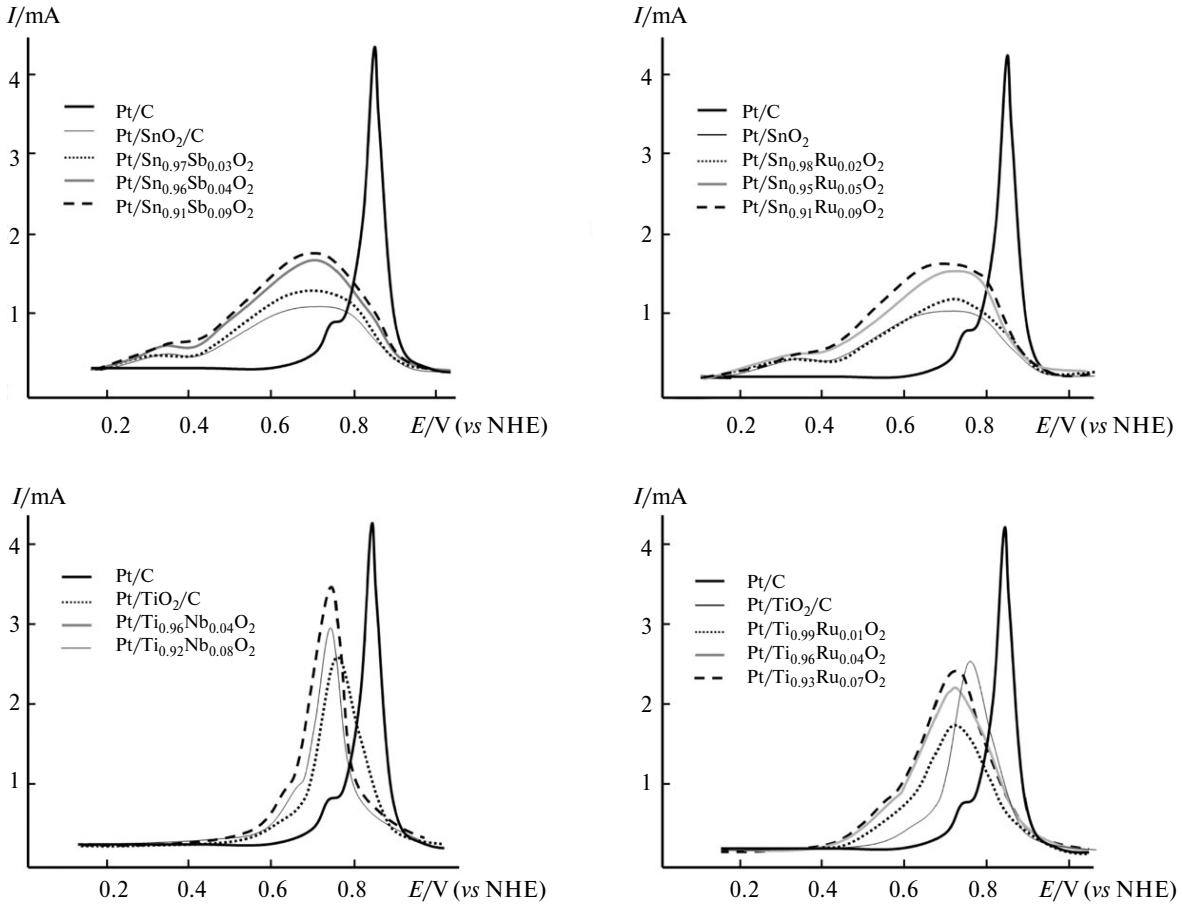

Fig. 6. Anodic parts of the CO-stripping voltammograms of the platinized oxides with various compositions. Base electrolyte 1 *M* H_2SO_4, $v = 0.05$ V s^{-1}.

A comparison of the potentiostatic polarization curves measured in the three-electrode electrochemical cell **1** for the platinized oxides with various compositions and for Pt(20%)/C and Pt(20%)Ru/C (E-TEK) during the oxidation of hydrogen mixtures with a carbon monoxide admixture content of 100 ppm is presented in Fig. 8.

The degree of resistance of the catalysts to poisoning with catalytic poisons (CO) can be estimated by the ratio $\Delta I/I$,

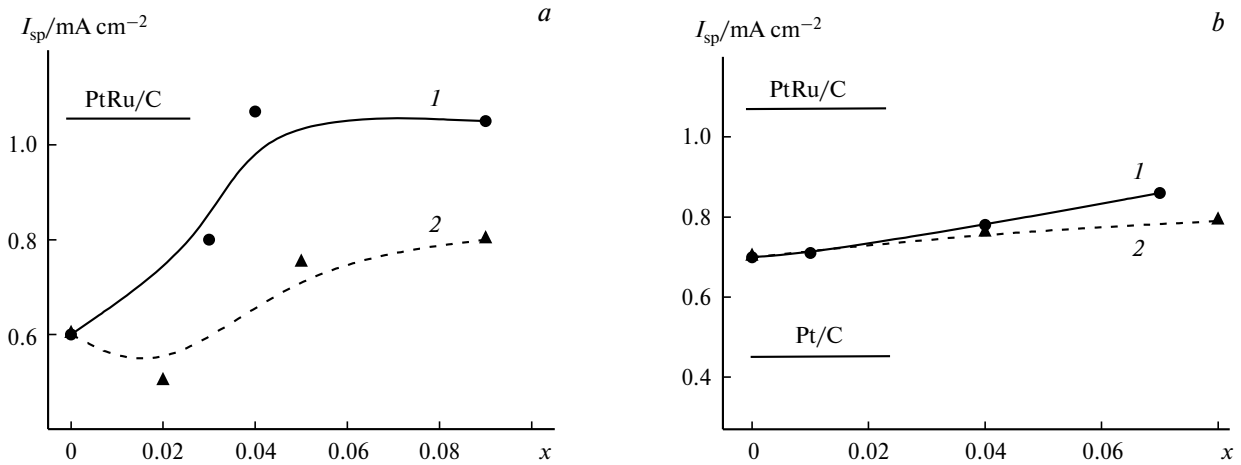

Fig. 7. Specific currents (I_{sp}) of the oxidation of the mixture (H_2/CO(100 ppm)) on the catalysts with various compositions: $Sn_{1-x}M_xO_2$ (*a*) with M = Sb (*1*) and Ru (*2*) and $Ti_{1-x}M_xO_2$ (*b*) with M = Nb (*1*) and Ru (*2*).

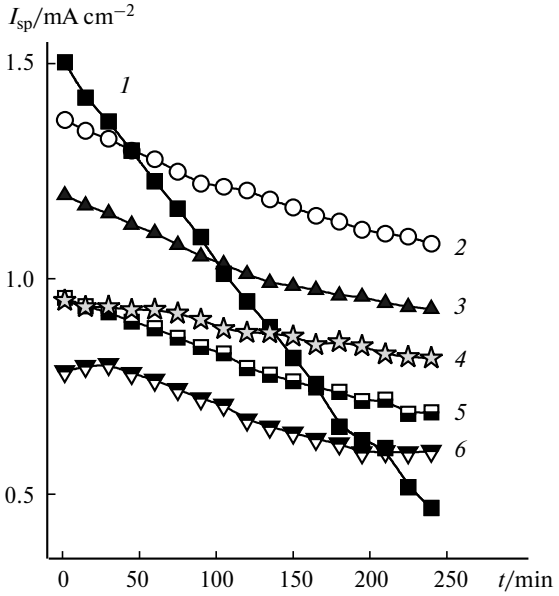

Fig. 8. Potentiostatic polarization curves for the platinized oxides with various compositions and Pt(20%)Ru/C and Pt(20%)/C (E-TEK) obtained by the oxidation of a mixture of hydrogen with the content of carbon monoxide admixture 100 ppm (E = 0.5 V): Pt/C (*1*), PtRu/C (*2*), $Pt/Sn_{0.91}Sb_{0.09}O_2$ (*3*), $Pt/Ti_{0.93}Ru_{0.07}O_2$ (*4*), Pt/TiO_2/C (*5*), and Pt/SnO_2/C (*6*).

where I is the oxidation current of the fuel at the initial moment, and ΔI is the current decrease within a certain time period. The corresponding values of $\Delta I/I$ calculated for the catalysts with various compositions are presented below.

Catalyst composition	$\delta I/I$
Pt/C	0.68
$Pt/Sn_{0.91}Sb_{0.09}O_2$	0.22
Pt/TiO_2/C	0.26
Pt/SnO_2/C	0.25
PtRu/C	0.20
$Pt/Ti_{0.93}Ru_{0.07}O_2$	0.15

It is seen that in long run tests the Pt-oxide catalysts showed a high stability of the catalytic activity of hydrogen oxidation in the presence of CO comparable with that of the commercial catalyst Pt(20%)Ru/C and the catalysts based on solid solutions turned out even more resistant to poisoning by carbon monoxide.

Electrocatalytic activity of the catalysts in the oxidation of methanol. The CV curves obtained in a MeOH solution for the catalytic systems based on individual oxides Pt/TiO_2/C and Pt/SnO_2/C and on solid solutions of various compositions are shown in Fig. 9 along with the data for the catalyst Pt(20%)/C (E-TEK) presented for comparison. The data show that the potentials of the oxidation peaks of methanol (I_{MeOH}) for Pt/MO_x are lower than those for platinum on the carbon support.

For the platinum catalysts supported on doped tin and titanium oxides, the shift of the peaks of I_{MeOH} is more pronounced than in the case of the corresponding individual oxides, and their intensity increases in the following order: $Pt/Sn_{1-x}Sb_xO_2$ (x = 0.04, 0.09) > $Sn_{1-x}Ru_xO_2$ (x = 0.05, 0.09) > $Ti_{1-x}Ru_xO_2$ (x = 0.07) > $Ti_{1-x}Nb_xO_2$ (x = 0.08). For the catalysts with a smaller amount of the introduced additives, the shifts of the peaks correspond to the values characteristic of individual oxides.

The values of specific currents obtained in the potentiostatic regime (E = 0.5 V) for the oxidation of a 0.5 M solution of MeOH with the catalysts of various compositions, including those measured in the presence of the system Pt(20%)Ru/C (E-TEK), are shown in Fig. 10. The dependence of the catalytic activity of the catalysts on the nature of the oxide of the support correlates with the results obtained by the study of the catalytic properties in hydrogen electrooxidation in the presence of CO. In the case of methanol electrooxidation, the amount of additives introduced into tin and titanium dioxides shows an effect not so evident as for hydrogen oxidation. Perhaps, the ohmic resistance of the support exerts a smaller effect

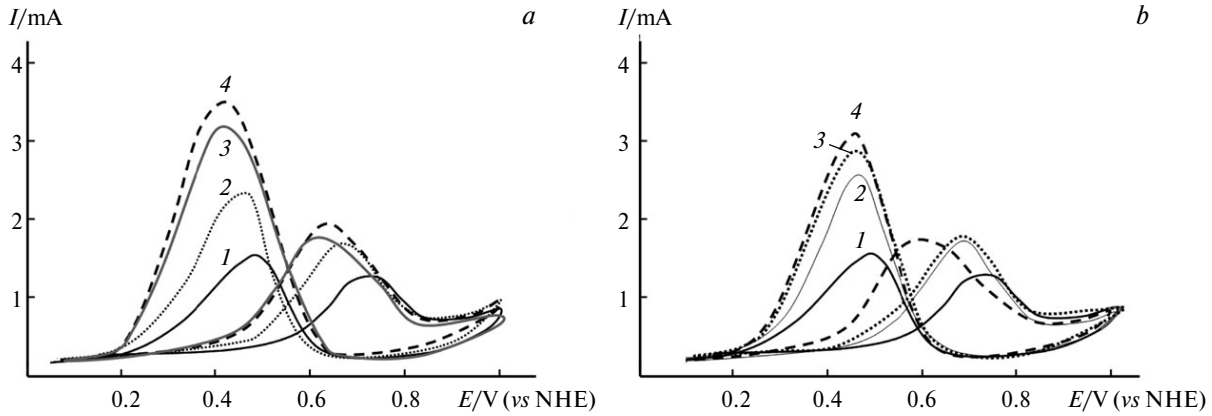

Fig. 9. Cyclic voltammograms of the catalysts $Pt/Sn_{1-x}M_xO_2$ (*a*) and $Pt/Ti_{1-x}M_xO_2$ (*b*) of various compositions and Pt(20%)/C (E-TEK) in 0.5 M CH_3OH; base electrolyte 1 M H_2SO_4, ν = 0.05 V s^{-1}. *a*: Pt/C (*1*), Pt/SnO_2/C (*2*), $Pt/Sn_{0.91}Ru_{0.09}O_2$ (*3*), and $Pt/Sn_{0.91}Sb_{0.09}O_2$ (*4*); *b*: Pt/C (*1*), Pt/TiO_2/C (*2*), $Pt/Ti_{0.92}Nb_{0.08}O_2$ (*3*), and $Pt/Ti_{0.93}Ru_{0.07}O_2$ (*4*).

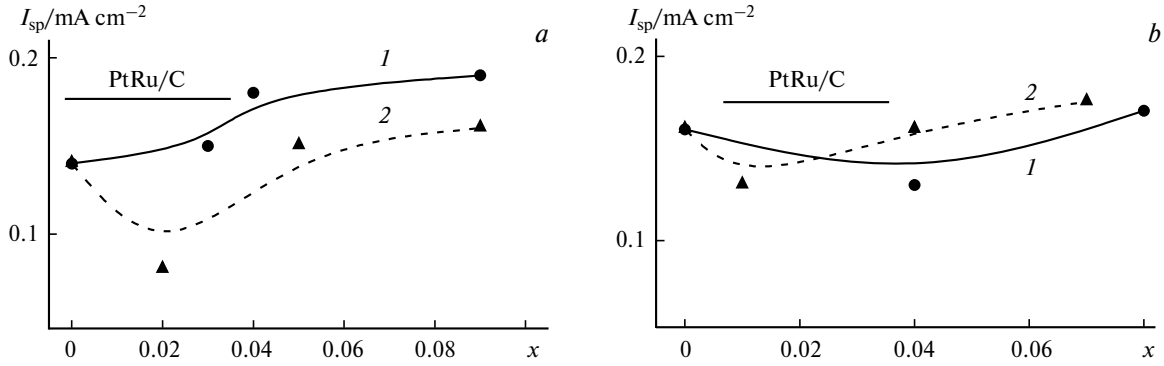

Fig. 10. Specific currents obtained by chronoamperometry (E = 0.5 V) on the catalysts with various compositions and Pt(20%)Ru/C (E-TEK) in 0.5 M CH_3OH: $Sn_{1-x}M_xO_2$ (*a*) with M = Sb (*1*) and Ru (*2*) and $Ti_{1-x}M_xO_2$ (*b*) with M = Nb (*1*) and Ru (*2*) Base electrolyte 1 M H_2SO_4.

on the process of methanol electrooxidation than that for the oxidation of H_2.

The values of exchange currents and slopes of the Tafel dependences (η—log*i*) for the reaction of MeOH oxidation are given in Table 4. The higher values of exchange currents (see Table 4, Fig. 11) indicate the easier electrooxidation of alcohol on the metal-oxide catalysts compared to that on Pt/C. The similarity of the Tafel curves for PtRu/C, Pt/TiO_2, Pt/SnO_2, and solid solutions based on them confirms that on the oxide catalysts the oxidation of methanol also follows the "bifunctional" mechanism (1), which is commonly accepted for the PtRu catalysts.[61]

Characteristics of the prototypes of the fuel cell with the catalyst $Pt/Sn_{0.91}Sb_{0.09}O_2$ at the anode of the membrane electrode assembly. The platinum catalyst based on $Sn_{0.91}Sb_{0.09}O_2$ was chosen for testing in the FC, because this catalyst is one of the most active among the systems studied. The operating characteristics of the hydrogen—air and methanol FC using the optimum compositions of the active layer of the anode $Pt/Sn_{0.91}Sb_{0.09}O_2$/Nafion[49] in the membrane electrode assembly are presented in Figs 12 and 13. The commercial catalyst Pt(20%)Ru/C (E-TEK) was used as a cathode. The voltammetric curves for the FC mounted according to the standard technologies using the commercial catalysts PtRu(20%)/C (E-TEK) at the anode and Pt(20%)/C (E-TEK) at the cathode are presented for comparison. Hydrogen with an additive of CO (100 ppm) was used for testing the hydrogen—air FC.

It was shown that the operating characteristics of the air and alcohol FC with the catalytic system $Pt/Sn_{0.91}Sb_{0.09}O_2$ at the anode were comparable with the characteristics of the FC based on the catalysts PtRu/C (E-TEK), indicating that the metal-oxide catalytic systems can be promising for use in hydrogen and methanol FC.

Thus, the electrocatalysts for the FC were prepared on the basis of individual platinized oxides Pt/SnO_2 and Pt/TiO_2 and their solid solutions $Pt/Ti_{1-x}M_xO_2$ (M = Ru, Nb) and $Pt/Sn_{1-x}M'_xO_{2-\delta}$ (M′ = Sb, Ru). The influence of the composition of the oxide supports on the activity of the supported Pt catalysts in the FC during the electrooxidation of MeOH and hydrogen in the presence of CO was studied.

The platinum electrocatalysts based on solid solutions of tin dioxide $Sn_{1-x}M'_xO_{2-\delta}$ (M′ = Sb, Ru; x = 0.4—0.9)

Table 4. Tafel slopes of the polarization curves and exchange currents (*i*) for the electrooxidation of methanol on various catalysts

Catalyst	$i \cdot 10^{-3}$/mA	∂E/∂log(*i*/mV)
Pt(20%)Ru/C	1.4±0.1	190
Pt(20%)/C	0.7±0.1	150
Pt/TiO_2	1.1±0.1	180
Pt/SnO_2	1.0±0.1	180
$Pt/Sn_{1-x}Sb_xO_2$ (x = 0.03—0.09)	1.3±0.1	180—190
$Pt/Sn_{1-x}Ru_xO_2$ (x = 0.03—0.09)	1.2±0.1	180—190
$Pt/Ti_{1-x}Ru_xO_2$ (x = 0.01—0.07)	1.1±0.1	150—160
$Pt/Ti_{1-x}Nb_xO_2$ (x = 0.4, 0.08)	1.0±0.1	155—170

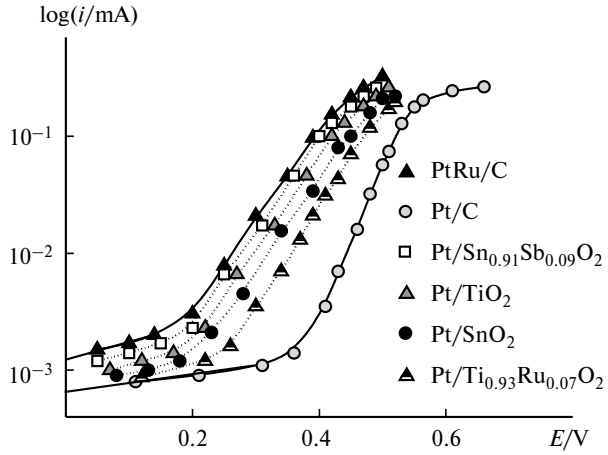

Fig. 11. Polarization curves in the logarithmic coordinates obtained for various catalysts in 0.5 M CH_3OH. The base electrolyte is 1 M H_2SO_4.

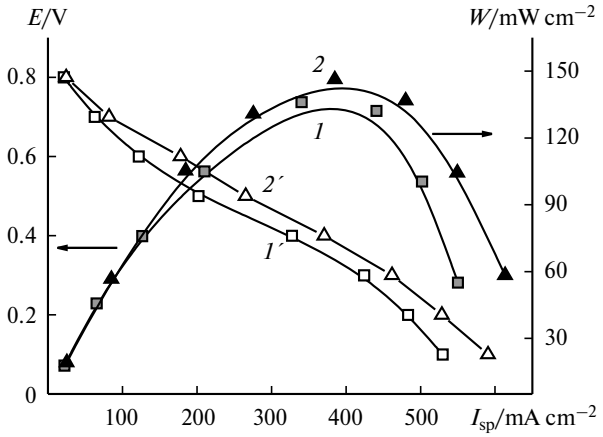

Fig. 12. Polarization curves (*1*, *2*) and power density of the MEA (*1′*, *2′*) in the hydrogen FCs with the catalysts at the anodes Pt(20%)Ru/C (E-TEK) (*1*, *1′*) and Pt(10%)/$Sn_{0.91}Sb_{0.09}O_2$ (*2*, *2′*). Fuel: H_2/CO(100 ppm), platinum loading at the electrodes 0.4 mg cm^{-2}, and temperature 25 °C.

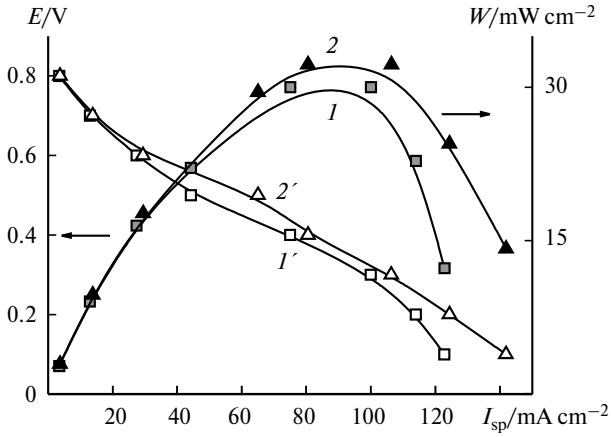

Fig. 13. Polarization curves (*1*, *2*) and power density of the MEA (*1′*, *2′*) in the methanol FCs (0.5 *M* MeOH) with the anode catalysts Pt(20%)Ru/C (E-TEK) (*1*, *1′*) and Pt(10%)/$Sn_{0.91}Sb_{0.09}O_2$ (*2*, *2′*). Platinum loading at the electrodes 1 mg cm^{-2}, and the temperature is 25 °C.

and titania $Ti_{1-x}M_xO_2$ (M = Ru, Nb; $x = 0.7$) are more resistant to poisoning with CO and are more active in alcohol electrooxidation than the commercial Pt,Ru catalysts on the carbon supports.

The tests of the novel platinized oxides incorporated in the hydrogen—air and methanol FCs showed higher power outputs of the FCs with the metal-oxide electrocatalysts at the anode compared to analogous energy systems based on the traditional Pt,Ru catalysts on the carbon supports.

This work was financially supported by the Ministry of Education and Science of the Russian Federation (State Contract No. 16.740.11.0251).

References

1. K.-Y. Chan, J. Ding, J. Ren, *Appl. Catal.*, 2003, **47**, 273.
2. K.-W. Park, J.-H. Choi, S.-A. Lee, C. Pak, H. Chang, Y.-E. Sung, *J. Catal.*, 2004, **224**, 236.
3. T. Kawaguchi, W. Sugimoto, Y. Murakami, Y. Takasu, *J. Catal.*, 2005, **229**, 176.
4. I.-S. Park, B. Choi, D.-S. Jung, Y.-E. Sung, *Electrochim. Acta*, 2006, **52**, 1683.
5. S.-A. Lee, K.-W. Park, B.-K. Kwon, Y.-E. Sung, *J. Ind. Eng. Chem.*, 2003, **9**, 63.
6. T. V. Parsons, *J. Electroanal. Chem.*, 1988, **257**, 45.
7. C. Lamy, A. Lima, V. LeRhun, F. Delime, C. Coutanceau, J.-M. Léger, *J. Power Sources*, 2002, **105**, 283.
8. P. J. Kulesza, K. Miecznikowski, B. Baranowska, *Electrochem. Commun.*, 2006, **8**, 5904.
9. S. Maass, F. Finsterwalder, G. Frank, R. Hartmann, C. Merten, *J. Power Sources*, 2008, **176**, 444.
10. S. Kotaro, S. Minhua, R. Adzic, *Polymer Electrolyte Fuel Cell Durability*, Springer, New York, 2009.
11. K. Kinoshita, *Carbon: Electrochemical and Physicochemical Properties*, Wiley, New York, 1988, p. 319.
12. B. Merzougui, S. Swathirajan, *J. Electrochem. Soc.*, 2006, **153**, 2220.
13. M. Cai, M. S. Ruthkosky, B. Merzougui, *J. Power Sources*, 2006, **160**, 977.
14. J. McBreen, H. Olender, S. Srinivasan, K. Kordesch, *J. Appl. Electrochem.*, 1981, **11**, 787.
15. G. R. Salazar-Banda, H. B. Suffredini, L. A. Avaca, S. A. S. Machado, *Mater. Chem. Phys.*, 2009, **117**, 434.
16. H.-J. Chun, D. B. Kim, D.-H. Lim, W.-D. Lee, H.-I. Lee, *Int. J. Hydrogen Energy*, 2010, **35**, 6399.
17. S. von Kraemer, K. Wikander, G. Lindbergh, A. Lundblad, A. E. C. Palmqvist, *J. Power Sources*, 2008, **180**, 185.
18. Y.-S. Lee, I.-S. Park, Y.-H. Cho, D.-S. Jung, N. Jung, H.-Y. Park, Y.-E. Sung, *J. Catal.*, 2008, **258**, 143.
19. M. S. Saha, R. Li, X. Sun, *Electrochem. Commun.*, 2007, **9**, 2229.
20. Y. Bai, J. Wu, X. Qiu, J. Xi, J. Wang, J. Li, W. Zhu, L. Chen, *Appl. Catal. B: Environmental*, 2007, **73**, 144.
21. L. Jiang, L. Colmenares, Z. Jusys, G. Q. Sunb, R. J. Behma, *Electrochim. Acta*, 2007, **53**, 377.
22. US Pat., *Conductive Matrices for Fuel Cell Electrodes*, 2006, 119 407; http://www.freepatentsonline.com/7767330.html.
23. US Pat., *Catalyst for Fuel Cell Electrode*, 2006, 124 248; http://www.wipo.int/pctdb/en/wo.jsp?WO=2006124248.
24. S. Kraemer, K. Wikander, G. Lindbergh, A. Lundblad, E. C. Anders, *J. Power Sources*, 2008, **180**, 185.
25. R. F. Bartholomew, D. R. Frankl, *Phys. Rev.*, 1969, **187**, 828.
26. D. Morris, Y. Dou, J. Rebane, C. E. J. Mitchell, R. G. Egdell, *Phys. Rev.*, 2000, **61**, 13445.
27. O. E. Haas, S. T. Briskeby, O. E. Kongstein, M. Tsypkin, R. Tunold, B. T. Børresen, *J. New Mater. Electrochem. Syst.*, 2008, **11**, 9.
28. B. Seger, A. Kongkanand, A. Vinodgopal, P. V. Kamat, *J. Electroanal. Chem.*, 2008, **621**, 198.
29. G. Y. Chen, S. R. Bare, T. E. Mallouk, *J. Electrochem. Soc.*, 2002, **149**, A1092.
30. K.-W. Park, K.-S. Seol, *Electrochem. Commun.*, 2007, **9**, 2256.

31. O. E. Haas, S. T. Briskeby, O. E. Kongstein, M. Tsypkin, R. Tunold, B. T. Børresen, *J. New Mater. Electrochem. Syst.*, 2008, **11**, 9.
32. B. L. García, R. Fuentes, J. W. Weidner, *Electrochem. Solid State Lett.*, 2007, **10**, B108.
33. L. A. Frolova, Yu. A. Dobrovolsky, N. G. Bukun, *Elektrokhimiya*, 2011, **47**, 697 [*Russ. J. Electrochem.* (*Engl. Transl.*), 2011, **47**, 745].
34. G. A. Tsirlina, Yu. E. Roginskaya, G. G. Postovalova, S. Yu. Vasil´ev, *Elektrokhimiya*, 1999, **35**, 1380 [*Russ. J. Electrochem.* (*Engl. Transl.*), 1999, **35**].
35. T. Okanishi, T. Matsui, T. Takeguchi, R. Kikuchi, K. Eguchi, *Appl. Catal., A*, 2006, **298**, 181.
36. Z. Liu, B. Guo, L. Hong, T. H. Lim, *Electrochem. Commun.*, 2006, **8**, 83.
37. L. Jang, L. Colmenares, Z. Jusys, G. Q. Sun, R. J. Behm, *Electrochim. Acta*, 2007, **53**, 377.
38. I. Saadeddin, B. Pecquenard, J. P. Manaud, R. Decourt, C. Labrugиre, T. Buffeteau, G. Campet, *Appl. Surf. Sci.*, 2007, **253**, 5240.
39. A. L. Santos, D. Profeti, P. Olivi, *Electrochim. Acta*, 2005, **50**, 2615.
40. K.-S. Lee, I.-S. Park, Y.-H. Cho, D.-S. Jung, N. Jung, H.-Y. Park, Y.-E. Sung, *J. Catal.*, 2008, **258**, 143.
41. W. J. Zhou, B. Zhou, W. Z. Li, Z. H. Zhou, S. Q. Song, G. Q. Sun, Q. Xin, S. Douvartzides, M. Goula, P. Tsiakaras, *J. Power Sources*, 2004, **126**, 16.
42. H. L. Pang, X. H. Zhang, X. X. Zhong, B. Liu, X. G. Wei, Y. F. Kuang, J. H. Chen, *J. Coll. Interface Sci.*, 2008, **319**, 193.
43. S. Lj. Gojkovic, B. M. Babić, V. R. Radmilović, N. V. Krstajic, *J. Electroanal. Chem.*, 2010, **639**, 161.
44. A. V. Smolin, B. I. Podlovchenko, *Elektrokhimiya*, 1998, **34**, 287 [*Russ. J. Electrochem.* (*Engl. Transl.*), 1998, **34**].
45. G. V. Shteinberg, I. A. Kukushkina, V. S. Bagotskii, M. R. Tarasevich, *Elektrokhimiya*, 1979, **15**, 527 [*Sov. Electrochem.* (*Engl. Transl.*), 1979, **15**].
46. O. Antoine, Y. Bultel, R. Durand, *J. Electroanal. Chem.*, 2001, **499**, 85.
47. Y. Bultel, L. Genies, O. Antoine, P. Ozil, R. Durand, *J. Electroanal. Chem.*, 2002, **527**, 143.
48. L. A. Frolova, Yu. A. Dobrovolsky, *Tr. III Mezhdunar. simp. po vodorodnoi energetike* [*Proceedings of the III International Symposium on Hydrogen Power Engineering*] *(Moscow, December 1—2, 2009*), Moscow, 2009, U-26 (in Russian).
49. L. A. Frolova, A. E. Ukshe, Yu. A. Dobrovolsky, *Al´ternativnaya energetika i ekologiya* [*Alternative Power Engineering and Ecology*], 2009, **76**, 151 (in Russian).
50. G. Qin, D. Li, Zh. Chen, Y. Hou, Zh. Feng, S. Liu, *J. Mater. Sci.*, 2009, **46**, 418.
51. D. R. M. Godio, J. Perez, H. M. Villullas, *J. Electrochem. Soc.*, 2007, **154**, B474.
52. X. M. Chen, G. H. Chen, P. L. Yue, *J. Phys. Chem.*, 2001, **105**, 4623.
53. Wang Aiping, X. U. Haibo, L. U. Yonghong, H. U. Jiezhen, K. Xiangfeng, T. Binglun, D. Hui, *Chin. J. Catal.*, 2009, **30**, 179.
54. M. D. Koninck, P. Manseau, B. Marsan, *J. Electroanal. Chem.*, 2007, **611**, 67.
55. E. M. Crabb, R. Marshall, D. Thompsett, *J. Electrochem. Soc.*, 2000, **147**, 4440.
56. F. A. Uribe, J. A. Valerio, F. H. Garzon, T. A. Zawodzinski, *Electrochem. Solid-State Lett.*, 2004, **7**, A376.
57. T. M. Koper, *Surf. Sci.*, 2004, **548**, 1.
58. C. Lu, C. Rice, R. I. Masel, P. K. Babu, P. Waszczuk, H. S. Kim, *J. Phys. Chem. B.*, 2002, **106**, 9581.
59. C. Lu, R. I. Masel, *J. Phys. Chem. B.*, 2001, **105**, 979.
60. T. Yajima, H. Uchida, M. Watanabe, *J. Phys. Chem. B.*, 2004, **108**, 2654.
61. S. Gilman, *J. Phys. Chem.*, 1964, **68**, 70.

Received March 4, 2011;
in revised form April 19, 2011